

An Approach to Analog Mitigation of RFI

Per Ödling, *Senior Member, IEEE*, Per Ola Börjesson, *Senior Member, IEEE*,
Thomas Magesacher, *Student Member, IEEE*, and Tomas Nordström, *Senior Member, IEEE*

Abstract—Among all noise sources present in wireline transmission systems we focus on one special type: narrowband radio frequency interference generated by radio amateurs (HAM) and broadcast radio stations. This disturbance, characterized by high power and narrow bandwidth, has the potential of overloading the receiver's analog-to-digital converter (ADC). Once the ADC is in saturation, any countermeasure taken in digital domain will fail. A viable way to face this problem is cancellation using the common-mode signal as a reference. This paper describes in detail an adaptive, mixed-signal, narrowband interference canceller employing a modified recursive least-squares algorithm, which is split into an analog and a digital part. The mixed-signal approach enables the circuit to generate an interference-cancelling signal of several MHz while operating the adaptive algorithm at some kilohertz. Simulation as well as measurement results show a steady-state disturbance suppression of about 35 dB. The convergence speed is high enough to protect the ADC from overloading due to time-variant HAM interference.

Index Terms—Cancellation, interference mitigation, radio frequency interference.

I. INTRODUCTION

EMERGING high-speed data transmission systems intended for use in the access part of the public telephony network, such as the digital subscriber line (xDSL) family, use a much larger bandwidth than the twisted copper pairs were originally intended for. This introduces impairments that researchers and engineers have not been faced with in voice-band modem technology. Among them radio frequency interference (RFI) is considered to be a real challenge. Wires, in particular the last meters to the subscriber as well as the inhouse wiring, act as antennas during broadband data transmission. They emit electromagnetic radiation which is referred to as *RFI ingress*. The radiation may disturb other services, in particular radio amateurs. Forced by legislation, the standardization obliges xDSL modems to reduce their transmit power within the frequency bands reserved for radio amateurs, the so called HAM-bands.

On the other hand, wires pick up radio signals from their environment, a phenomenon referred to as *RFI ingress*. Two main

sources are broadcast radio stations and amateur radio transmitters (HAM transmitters). Especially the interference from radio amateurs is difficult to handle. It is nonstationary, as the transmission is intermittent and bursty, and exhibits potentially high power levels when transmitters are close to the wiring. The effect of HAM interference could be compared with having somebody shouting in your ear while trying to listen to a polite conversation. Broadcast radio stations are easier to cope with since they transmit continuously and are, most often, not as close to twisted pair wires as amateur radio transmitters.

A considerable amount of work on mitigating RFI ingress has already been done, partly driven by the very high-speed digital subscriber line (VDSL), asymmetric digital subscriber line (ADSL), and single-pair, symmetric digital subscriber line (SDSL) standardization processes. A basic overview of the interference problem in xDSL is provided in [1]. Investigations of the RFI environment, as well as practical ingress measurement results can be found in [2]–[4]. Mitigation techniques in the digital domain, i.e., after the analog-to-digital converter (ADC), are often different for multicarrier modulation (MCM) and single-carrier modulation (SCM). There are several ways to cope with RFI in discrete multitone (DMT) based MCM transmission: filtering, windowing, and digital RFI cancellation [5]–[8]. In SCM, the decision feedback equalizer (DFE) is often the key element concerning narrowband interference mitigation. Investigations can be found in [9] and [10]. All digital RFI mitigation techniques work as long as the receiver's ADC is not overloaded. Short-time clipping events may, depending on their duration, be handled by an interleaver/deinterleaver present in the system. Strong radio frequency interference, however, can generate a lasting overload condition which must be avoided.

The purpose of this paper is to detail a theoretical approach, and describe a corresponding implementation, to mitigate strong narrowband RFI in the analog domain, i.e., before the modem's ADC. Cancellation for time division duplexing systems, making use of the silent period between changes of transmission direction, has been proposed in [11]. A similar solution, implemented in an analog front-end for VDSL, has been reported in [12]. Our approach is capable of suppressing intermittent HAM disturbance quickly enough to prevent overload conditions also in systems applying frequency division duplexing. These results have in part been presented in [13].

The paper is organized as follows. Section II analyzes the RFI ingress problem. Models for the interference and the coupling process are derived. Section III introduces the canceller. Its adaptation is done by a modified RLS algorithm exploiting the narrowband property of the disturber. A detailed derivation of the algorithm is given in the Appendix. Implementation aspects, especially addressing the analog part, are also discussed.

Manuscript received May 6, 2001; revised January 3, 2002.

P. Ödling is with the Telecommunications Research Center, Vienna (FTW), Austria and also with the Lund Institute of Technology, Department of Applied Electronics, Se 221 00 Lund, Sweden.

P. O. Börjesson is with the Lund Institute of Technology, Department of Applied Electronics, Se 221 00 Lund, Sweden.

T. Magesacher is with Infineon Technologies, A-95000 Villach, Austria and also with the Institute for Integrated Circuits at Munich Technical University, Germany.

T. Nordström is with the Telecommunications Research Center, Vienna (FTW), A-1220 Vienna, Austria.

Publisher Item Identifier S 0733-8716(02)05380-5.

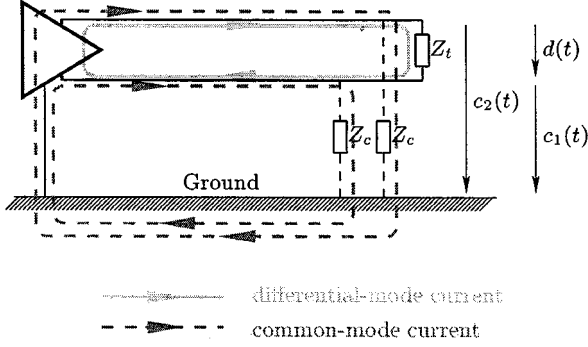


Fig. 1. DM and CM currents and voltages in wireline transmission.

An evaluation of the circuit is done by simulations in Section IV. The principle has been verified by experimental results presented in Section V.

II. RADIO FREQUENCY INTERFERENCE

A. RFI Ingress

The signal we wish to transmit is applied as a voltage between two wires causing a differential-mode (DM) current, as depicted in Fig. 1. Any radio frequency interferer located closely enough to the wire will cause RFI ingress due to electromagnetic coupling. When talking about RFI ingress, two types should be distinguished. First, the interference will cause an additional DM current in the loop formed by the two wires. The DM signal $d(t)$ at the termination impedance Z_t consists of the desired signal $s(t)$, the narrowband disturbance component $r(t)$, and a noise $v_d(t)$, i.e.,

$$d(t) = s(t) + r(t) + v_d(t). \quad (1)$$

The disturbance $r(t)$ interferes additively with the desired signal $s(t)$ and should be kept as low as possible in order not to saturate the receiver's ADC. Shielded cables would be the preferred choice, but they are rarely installed in the access network. Twisting the two wires lowers the ingress substantially, since the induced currents change their direction from twist to twist and cancel themselves to a certain extent.

Second, RFI ingress will also appear in the loops formed by each of the two wires and ground. These loops are closed by the coupling impedances Z_c . Their values depend on a variety of parameters, for example the type of the cable, its position relative to ground, the hybrids used for two-wire to four-wire conversion, etc. These common-mode (CM) currents find their return path via ground. The resulting CM signal $c(t) = (c_1(t) + c_2(t))/2$ may be obtained by the center tap of a transformer and primarily consists of the disturbance caused by radio ingress. In general, the CM interference will be much larger than its corresponding DM component since the CM loops have larger areas and are, thus, more susceptible to RFI. Due to unbalance of the wire pair and the transformer, $c(t)$ may also contain a small portion of the desired signal. In practice, however, the amount of interference will be substantially higher than the desired signal component.

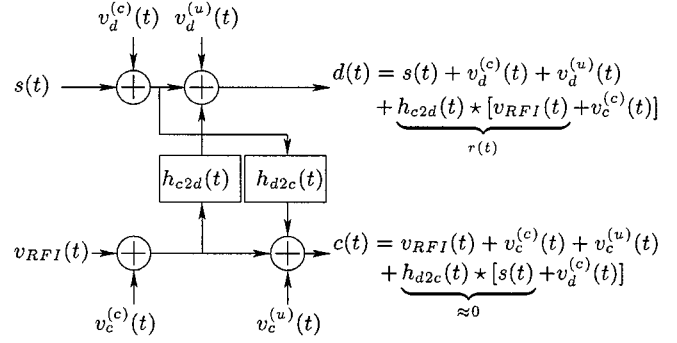


Fig. 2. Signals and coupling model between DM and CM.

B. Signal and Coupling Models

Based on the observations made at physical layer in the previous section, we identify the general coupling model depicted in Fig. 2. The coupling impulse responses from DM to CM and vice versa are denoted by $h_{d2c}(t)$ and $h_{c2d}(t)$, respectively, and \star is the convolution operator. The DM output signal $d(t)$ consists of the desired signal $s(t)$, a noise component $v_d^{(c)}(t) + h_{c2d}(t) \star v_c^{(c)}(t)$, which is correlated with the CM output signal $c(t)$ due to the two signal coupling paths, an additional noise component $v_d^{(u)}(t)$, and the RFI component $r(t)$. Analogously, the CM signal $c(t)$ is made up of the narrowband disturber $v_{RFI}(t)$, a noise component $v_c^{(u)}(t)$ uncorrelated with the DM output signal $d(t)$, a correlated part $v_c^{(c)}(t) + h_{d2c}(t) \star v_d^{(c)}(t)$, and the signal component $h_{d2c}(t) \star s(t)$. The coupling between CM and DM and vice-versa is linear but frequency dependent. As discussed before, the CM interference $v_{RFI}(t)$ is generally much stronger than the signal $s(t)$. Note that, as our canceller uses the CM $c(t)$ as a reference signal, having a desired-signal component at the CM input might, in principle, cause the canceller to eliminate the differential-mode desired signal. But since the purpose of analog RFI mitigation is to address the case where $v_{RFI}(t)$ is strong, we will neglect the DM to CM coupling of the signal, thus, $c(t) = v_{RFI}(t) + v_c(t)$, where $v_c(t) = v_c^{(c)}(t) + v_c^{(u)}(t) + h_{d2c}(t) \star v_d^{(c)}(t)$ represents the total noise at the CM input. Taking into account that the RFI disturber $v_{RFI}(t)$ is of very narrow bandwidth, i.e., essentially sinusoidal, the coupled RFI $h_{c2d}(t) \star v_{RFI}(t)$ turns into

$$r(t) = 1/a_{c2d} c(t + \tau_{lag}). \quad (2)$$

The DM interference $r(t)$ is virtually the same as the CM signal $c(t)$, except that it is scaled by $1/a_{c2d}$ and shifted in time by τ_{lag} .

Depending on the type of wire, the CM to DM coupling can be as high as $a_{c2d, dB} = 30$ dB, i.e., the attenuation from CM to DM is 30 dB. The CM disturbance can be in the order of 30 V_{peak} at the receiver, which may result in DM disturber levels of up to 0.5 V_{peak} [2], [3]. The level of the desired signal at the receiver's input, for a medium wire length of 1.5 km, is typically in the range of 60–80 mV_{peak}. The receiver's ADC is normally tuned to sample only the desired signal. In the presence of strong RFI, the ADC will then saturate, and the desired signal is lost.

The most broadband xDSL system so far is VDSL, which uses up to 12 MHz. There are several HAM bands used by

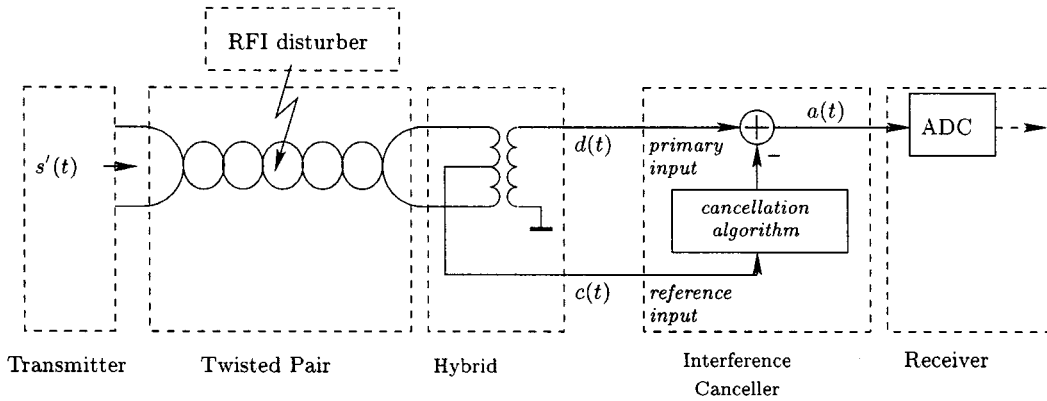


Fig. 3. Principle of analog RFI cancellation.

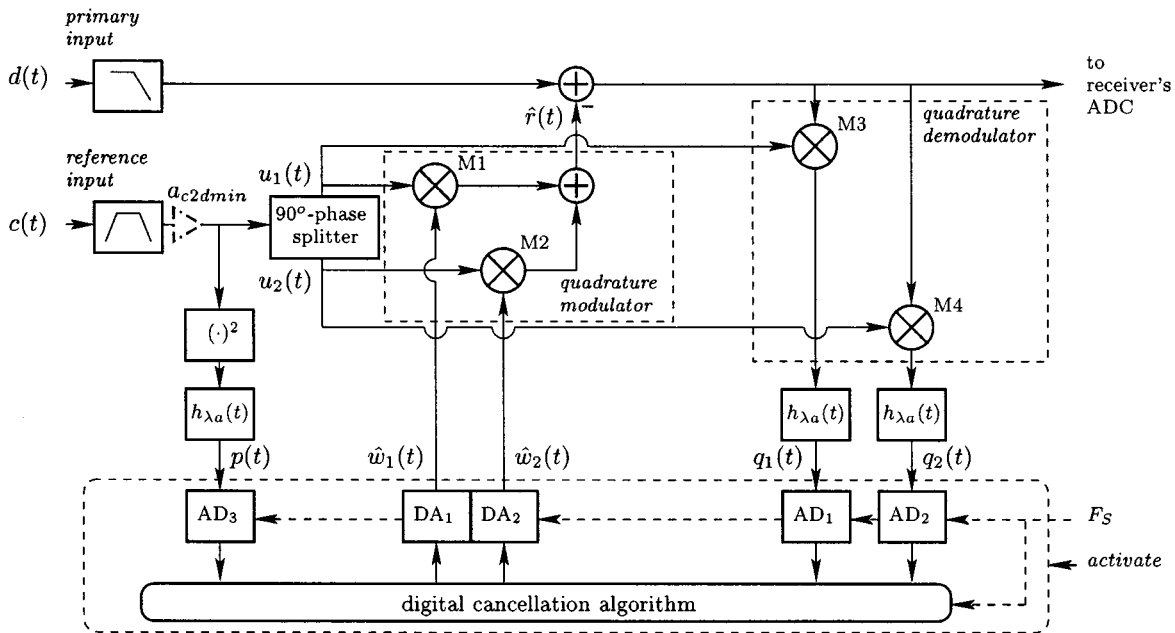


Fig. 4. Canceller block diagram.

radio amateurs that lie between 1 MHz and 12 MHz. The bands themselves are well defined but within them the radio amateur transmitter may change its transmit frequency arbitrarily. Although the carrier frequencies are high, the maximum bandwidth of the disturbing signals is only some kilohertz, as defined by national and international regulations. What we really need to track with the canceller are changes in the coupling from the CM signal to the DM signal, i.e., a_{c2d} and τ_{lag} in (2) as functions of time. They are both frequency dependent and will change when the RFI disturber changes its frequency. However, their change is virtually zero within the few kilohertz of bandwidth of a HAM-disturber. Neither does the disturber traverse along the line at any speeds that would cause rapid changes in the coupling. Thus, in practice we can assume that a_{c2d} and τ_{lag} are constant for a given RFI disturber.

III. COMMON-MODE REFERENCE BASED CANCELLER

The principle of analog RFI cancellation using the CM signal as a reference is illustrated in Fig. 3. The fact that the disturbing

signal is of special nature, i.e., of small bandwidth, can be utilized when designing a canceller [14]. We use a combination of high-frequency analog signal processing and low-frequency digital signal processing. Our adaptive canceller is based on a modified RLS algorithm which is split into one analog and one digital part.

A. Signal Decomposition

Fig. 4 shows a block diagram of the canceller. The analog-to-digital and digital-to-analog converters (ADCs and DACs) operate at the sampling frequency F_s , which corresponds to the algorithm's update rate and is relatively low as we will see. As illustrated in Figs. 3 and 4, the circuit has two inputs: a primary input for the DM signal $d(t)$ and a reference input for the CM signal $c(t)$. Every $T = 1/F_s$ seconds, the cancellation algorithm calculates a new coefficient vector

$$\hat{w}[n] = \begin{bmatrix} \hat{w}_1[n] \\ \hat{w}_2[n] \end{bmatrix}, \quad n = 0, 1, \dots \quad (3)$$

which is converted into the time-continuous weight signals $\hat{w}_1(t)$ and $\hat{w}_2(t)$ by the two DACs in Fig. 4, i.e.,

$$\hat{\mathbf{w}}(t) = \begin{bmatrix} \hat{w}_1(t) \\ \hat{w}_2(t) \end{bmatrix} = \hat{\mathbf{w}}[n], \quad nT \leq t < (n+1)T. \quad (4)$$

The CM signal $c(t)$ serves as a reference and is converted into two orthogonal signals, collected in the vector

$$\mathbf{u}(t) = \begin{bmatrix} u_1(t) \\ u_2(t) \end{bmatrix} \quad (5)$$

by means of a 90°-phase splitter. The elements of $\mathbf{u}(t)$ are weighted by $\hat{\mathbf{w}}(t)$ to generate the interference-cancelling signal

$$\hat{r}(t) = \hat{\mathbf{w}}^T(t)\mathbf{u}(t) \quad (6)$$

where $(\cdot)^T$ denotes the transpose. Note that (6) is realized by the quadrature modulator in Fig. 4. With the two parameters $\hat{w}_1(t)$ and $\hat{w}_2(t)$, both amplitude and phase of the sinusoidal interference-cancelling signal $\hat{r}(t)$ can be arbitrarily adjusted. The resulting *a priori* estimation error is given by

$$\xi(t) = d(t) - \hat{r}(t). \quad (7)$$

The quadrature demodulator generates the two-component, baseband, error signal $\mathbf{q}(t)$, which is the lowpass-filtered product of $\mathbf{u}(t)$ and the *a priori* estimation error $\xi(t)$ caused by the current weight vector, i.e.,

$$\mathbf{q}(t) = \begin{bmatrix} q_1(t) \\ q_2(t) \end{bmatrix} = h_{\lambda a}(t) \star (\mathbf{u}(t)\xi(t)) \quad (8)$$

where $h_{\lambda a}(t)$ is the impulse response of the two right-most lowpass filters of Fig. 4. The optimum choice of the impulse response will be derived in the sequel. We assume that the interference $r(t)$ and the desired signal $s(t)$ are uncorrelated, which holds in practice. Furthermore, the following measure of the CM reference signal power

$$p(t) = h_{\lambda a}(t) \star c(t)^2 \quad (9)$$

will be essential for both the weight-updating and detecting the presence of a disturber, again using a lowpass filter with impulse response $h_{\lambda a}(t)$. The signals $q_1(t)$, $q_2(t)$, and $p(t)$ are then sampled at the rate F_s by three ADCs. Since each of these three signals is essentially a lowpass-filtered product of sinusoids having the same frequency, we can interpret them as down-converted, DC-like signals. The canceller has to track only these slowly varying levels, thus, the sampling frequency F_s of the converters can be in the range of only some kilohertz.

B. Formulation of the Adaptive Algorithm

The small bandwidth of the interferer allows the introduction of the following model for the DM signal:

$$d(t) = \mathbf{w}_o^T(t)\mathbf{u}(t) + s(t) + v_d(t) \quad (10)$$

where $\mathbf{w}_o(t) = [w_{o,1}(t)w_{o,2}(t)]^T$ is the true unknown weight vector. Any noise present at the receiver's input is represented by $v_d(t) = v_d^{(c)}(t) + v_d^{(u)}(t) + h_{c2d}(t) \star v_c^{(c)}(t)$ (cf. Fig. 2).

We aim at finding an updated estimate $\hat{\mathbf{w}}[n]$ given an estimate $\hat{\mathbf{w}}[n-1]$ at iteration $n-1$, as well as the observable signals $\mathbf{u}(t)$ and $d(t)$. Note that this problem is similar to the classical recursive least-squares (RLS) algorithm [15] albeit there are two differences. First, our model is not based on a transversal filter since $\mathbf{u}(t)$ does not represent a tap vector. Second, the observable signals $\mathbf{u}(t)$ and $d(t)$ are time-continuous. Hence, we define the cost function

$$\mathcal{E}[n] = \frac{1}{T} \int_0^{nT} \lambda^{(nT-t)/T} e^2(t) dt \quad (11)$$

where

$$e(t) = d(t) - r(t) \quad (12)$$

is the estimation error and the constant $\lambda < 1$ is a forgetting factor weighting recent data higher and older data lower. We introduce two assumptions here. First, assume that $u_1(t)$ and $u_2(t)$ have the same time-averaged power [cf. (32, Appendix)]. Second, since the reference-signal components $u_1(t)$ and $u_2(t)$ are orthogonal, we assume that their time-averaged product is zero [cf. (33, Appendix)]. Minimizing (11) yields the update rule for the weight vector,

$$\hat{\mathbf{w}}[n] = \hat{\mathbf{w}}[n-1] + \frac{1}{P[n]} \mathbf{q}(nT) \quad (13)$$

with

$$P[n] = \lambda P[n-1] + p(nT). \quad (14)$$

Equations (13) and (14) constitute the digital part of the update algorithm. The analog part comprises the weighting within one period T , carried out by the three lowpass filters in (8) and (9). By minimizing (11), we obtain the optimum lowpass filter impulse response

$$h_{\lambda a}(t) = \begin{cases} \frac{1}{T} \lambda^{t/T}, & 0 \leq t \leq T \\ 0, & \text{otherwise.} \end{cases} \quad (15)$$

The derivation of the algorithm is given in full in the Appendix.

C. Implementation Aspects

Each component of the analog part, including the ADCs and DACs, will introduce noise as well as offsets. From a system point of view, the canceller can be seen as an additional broadband noise source located between the line and the receiver. Its contribution to the total noise present at the receiver's input should not lower the overall performance. Our experience from building low-cost demonstrators shows that especially the multipliers M1 and M2 in Fig. 4 should be designed carefully since their output directly affects the output signal of the canceller. However, several examples show that high quality integration of similar circuits is possible [16], [17].

The 90°-phase splitter can be realized by a phase locked loop (PLL), which is also the case in our demonstrator used in Section V. One output of the splitter is identical to the input, i.e., $u_1(t) = c(t)$, and the other output $u_2(t)$ is the PLL output signal. The circuit can handle slow changes of the disturber's frequency, corresponding to low bandwidth.

1) *Offset Compensation*: The offsets present in the circuit can be compensated for to a certain extent. The compensation is done in two steps. First, setting both inputs $c(t)$ and $d(t)$ as well as the weights to zero, all three canceller input signals should be zero as well. The values measured in this state are the input offset levels. The input signals are corrected by subtracting these levels from this point on. Second, a sinusoid at the reference input is provided while the DM input signal as well as the weights are still kept zero. Ideally, the canceller output should be zero, but due to DAC offsets there may be some CM leakage. If we start the canceller now, it will eliminate this leakage—the resulting weight values correspond to the negative offset levels of the DA-converters. These should be the starting weights $\mathbf{w}[n]$ when the canceller is turned on in order to avoid transients. During the measurements, reported in Section V, we employ these compensation procedures.

2) *Low-Pass Filter*: Realizing the optimum lowpass filter (15) exclusively in analog domain is rather expensive. We suggest a mixed-signal implementation, yielding exactly the same functionality by splitting the filter into a first-order analog low-pass followed by a first-order digital filter [18]. Generally, (15) can be approximated by a first-order analog lowpass only, potentially yielding similar results. However, the choice of the cutoff frequency would have to be made heuristically, whereas the derivation given in Section III-B and in the Appendix provides the parameters needed for optimum filter design.

3) *Converter Resolution*: The canceller needs three ADCs and two DACs. As discussed in Section III-A, it is sufficient to choose the sampling frequency F_s to be only some kilohertz in the VDSL environment. This is about a 1000 times lower than the receiver's ADC sampling frequency.

The canceller's input and output signals are of low bandwidth. Thus, the required converter resolution can be determined by a static analysis. The level difference a_{c2d} between CM and DM can partly be compensated for by a fixed attenuation $a_{c2d\min}$ at the CM input. The remaining part $\Delta a_{c2d} = a_{c2d}/a_{c2d\min}$, which depends on the balance variation of the cables the canceller is designed for, has to be realized by the coefficients.

In steady-state, each of the two DACs generates a coefficient ranging between normalized values of -1 to 1 , with a maximum error $\Delta w \approx 2^{-N_{\text{DA}}}$, where N_{DA} is the resolution. An RFI disturber of level V_{RFI} at the DM input will cause a residual interferer of amplitude $V_{\text{RFI}}\Delta a_{c2d}\sqrt{2}\Delta w$ at the canceller output. Thus, the achievable RFI suppression ΔSIR is limited by $\Delta SIR \leq 2^{N_{\text{DA}}}/(\sqrt{2}\Delta a_{c2d})$, consequently yielding $N_{\text{DA}} \geq \log_2(\sqrt{2}\Delta a_{c2d}\Delta SIR + 1)$. A desired suppression of 40 dB for a coupling factor variation of $\Delta a_{c2d,\text{dB}} = 30$ dB requires $N_{\text{DA}} = 13$.

The resolution of AD_1 and AD_2 is determined by the ratio of their maximum input level $V_{\text{RFI}}^2 a_{c2d}$ and their minimum input level of interest $V_{\text{RFI}}^2 a_{c2d}/\Delta SIR$, i.e., $N_{\text{AD}12} \geq \log_2(2\Delta SIR)$. Thus, $N_{\text{AD}12} = 8$ is sufficient for an RFI suppression level of 40 dB.

AD_3 essentially has to cope with the range of the coupling factor, i.e., $N_{\text{AD}3} \geq 2\log_2(\Delta a_{c2d})$, which yields $N_{\text{AD}3} = 10$ for $\Delta a_{c2d,\text{dB}} = 30$ dB.

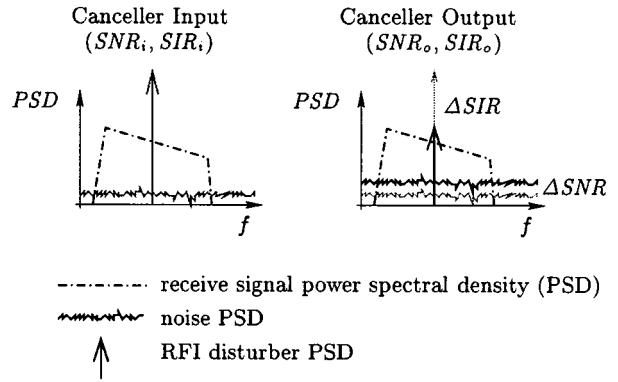


Fig. 5. Performance measures in steady-state: RFI suppression ΔSIR and SNR loss ΔSNR .

To summarize, the resolution of the canceller's converters are between, say, 8 to 13 bits and the bandwidth of the converters is in the kilohertz range.

D. Performance Measures

The quality of the adaptive canceller can be measured by three parameters. Two of them describe the performance in steady state, i.e., when the algorithm has converged and the coefficients are frozen. Fig. 5 depicts the situation in terms of power spectral density (PSD). We denote the ratio of signal power P_s to noise power $P_{n,d}$ at the canceller input as SNR_i and the ratio of signal to RFI power ($P_s/P_{\text{RFI},d}$) as SIR_i . The canceller will suppress the disturber by ΔSIR , yielding a (higher) signal to RFI ratio SIR_o at its output. However, the canceller may also introduce broadband noise for two reasons. First, the implementation of the analog part is crucial from a noise point of view, as discussed in the previous section. Second, broadband noise $v_c(t)$, present at the CM input, is treated the same way as the RFI reference signal $v_{\text{RFI}}(t)$, i.e., $v_c(t)$ is weighted by the coefficients and added to $d(t)$. This effect represents an additional noise source, although $v_c(t)$ is attenuated by approximately a_{c2d} , assuming equal CM to DM and DM to CM coupling behavior. Thus, SNR_i may be reduced by ΔSNR to the signal to noise power ratio at the canceller output SNR_o . RFI suppression ΔSIR together with the SNR loss ΔSNR characterize the performance in steady state.

The third parameter is the time or, equivalently, the number of iterations, which the canceller needs to attain a certain RFI suppression ΔSIR .

E. Performance Requirements

Mitigation of strong RFI should be done both in analog and digital domain. The purpose of an analog canceller is to lower the requirements on the precision of the analog receiver circuitry, in particular the resolution of the ADC, to a reasonable measure. The residual RFI can then be countered in the digital domain.

The RFI suppression that is necessary to protect the receiver's ADC from overloading, depends on the operating point of the modem, i.e., the power levels of signal, disturber and noise. Furthermore, there is a tradeoff between the precision of the receiver's ADC and the required level of suppression, as discussed

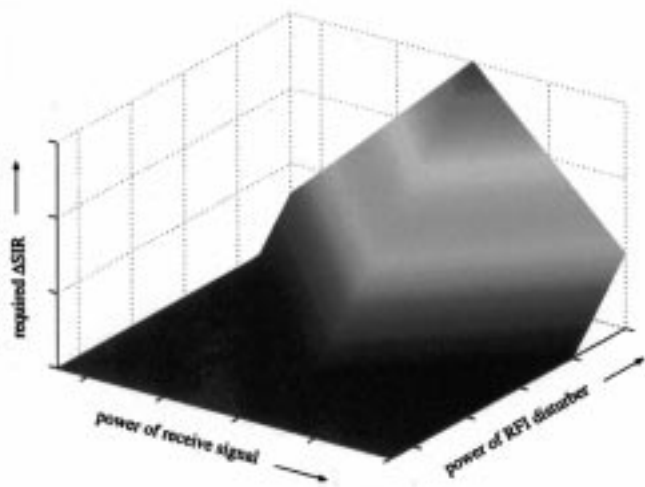


Fig. 6. RFI suppression ΔSIR required to reduce the RFI power to be equal to the desired-signal power.

in the following. The analog front-end (AFE) of a DSL receiver usually employs a programmable-gain amplifier before the receiver’s ADC to handle the high dynamic range of the input signal. An unmodulated RFI disturber has a peak-to-average ratio (PAR) of 3 dB. The desired signal’s PAR is 14–18 dB depending on the modulation type [19]. Assume the analog canceller reduces the power of a strong RFI disturber to be equal to the power of the desired signal. The peak level of the disturber will be 11 dB, or equivalently 3.55 times, lower than the peak level of the signal. Thus, an additional effective resolution of 0.35 bit is required for clipping-free AD conversion of a desired signal disturbed by RFI of the same power. The RFI suppression required to avoid an ADC overload condition is depicted qualitatively in Fig. 6. In general, a certain RFI suppression level is necessary to sufficiently suppress the maximum power RFI in case of maximum desired-signal level (east corner of Fig. 6). If we now move from this point in the plot towards decreasing desired signal power, it makes sense to increase the programmable gain if the noise level at the DM input is below the internal AFE noise floor, which depends mainly on the receiver’s ADC and determines the SNR in that case. Since the RFI disturber is amplified as well, the required ΔSIR rises. At a certain desired-signal level, further increase of the programmable gain is no longer advantageous, since the DM input noise level would rise above the internal noise floor. From that point on we gain headroom decreasing the desired signal power, which enables us to handle the interferer and consequently reduce the required ΔSIR .

Increasing the ADC resolution lowers the required RFI suppression ΔSIR and vice-versa. The performance tradeoff between receiver’s ADC and analog RFI canceller corresponds to shifting the surface along the $z(\Delta SIR)$ axis.

The loss of SNR due to the canceller, characterized by ΔSNR , should be kept as low as possible. During the adaptation phase, the weighting coefficients and, thus, the residual RFI at the canceller output change step-wise, which may cause transient noise. However, many standardized DSL systems, including VDSL, use an error correcting code together with an interleaver. This allows bursty disturbance of several 100 μs

TABLE I
SUMMARY OF RFI-RELEVANT PARAMETERS AND THEIR RANGES USED IN THE SIMULATIONS (BANDWIDTH OF ANALOG INPUT SIGNALS: 12 MHz)

parameter	symbol	range	unit
Signal power at DM input	P_s	-55 ... 10	dBm
RFI power at DM input	$P_{RFI,d}$	$\min(P_s) \dots 0$	dBm
Noise power at CM input (flat)	$P_{n,c}$	-70 ... -5 + a_{c2d}	dBm
Noise power at DM input (flat)	$P_{n,d}$	-70 ... -5	dBm
CM to DM and DM to CM attenuation	$a_{c2d,dB}$	30 ... ∞	dB
RFI bandwidth	B_{rfi}	$\approx 0^1 \dots 7$	kHz

¹Corresponds to an unmodulated tone in steady state. However, during ramp-up the bandwidth is not zero, since the amplitude rises from zero to full scale.

duration, which is sufficient to protect the transmitted data at the time instants the coefficients change. As soon as the canceller reaches the required RFI suppression, the coefficients can be frozen and updated at a much lower frequency.

In order to protect the receiver’s ADC from overloading, an emerging RFI interferer has to be detected and tracked early enough. Due to their limited bandwidth, HAM signals need approximately 1 ms to reach their nominal power. Within this ramp-up time, the required ΔSIR must be achieved.

IV. SIMULATIONS

A. Parameters

Adaptive cancellation of RFI in DSL systems spans a simulation parameter space of considerably large dimensionality. Table I summarizes the parameters relevant for RFI. The given minimum and maximum values indicate the ranges that real (V)DSL systems typically operate in, as will be discussed in the following.

The power of a VDSL modem’s transmit signal is limited as standardization allows a maximum transmit power and a maximum PSD of 10 dBm and -60 dBm/Hz, respectively [20], [21]. The desired signal’s PSD is determined by the loop’s attenuation. A reasonable lower bound for DM and CM noise PSDs is given by the white Gaussian noise floor of -140 dBm/Hz. Broadband noise at the DM input includes crosstalk, which is often the performance limiting noise source. We restrict our considerations to cases where $SNR_i > 15$ dB, since this is the minimum required SNR for the modulation types used in DSL [22]. Because of that the maximum DM noise power is -5 dBm and the minimum desired signal power is approximately -55 dBm, assuming a bandwidth of 12 MHz. The CM noise that leaks to the canceller output is attenuated by a factor a_{c2d} due to the weighting coefficients. Thus, we chose the maximum CM noise to be a_{c2d} times stronger than the maximum desired signal. The maximum RFI power at the DM input is 0 dBm according to the standard. As discussed before, we focus on strong RFI ingress, i.e., the lower limit is the DM signal power of the corresponding scenario. The coupling of a narrowband signal from CM to DM can be described by a complex frequency domain coefficient corresponding to the attenuation a_{c2d} and a delay. The CM to DM attenuation ranges from 30 dB for untwisted cables to infinity for theoretically perfect cables. Coupling of the broadband DM signal to CM is frequency dependent. For the sake of simplicity, we assume flat coupling. The special case where the coupling is strong in a certain frequency range within the band

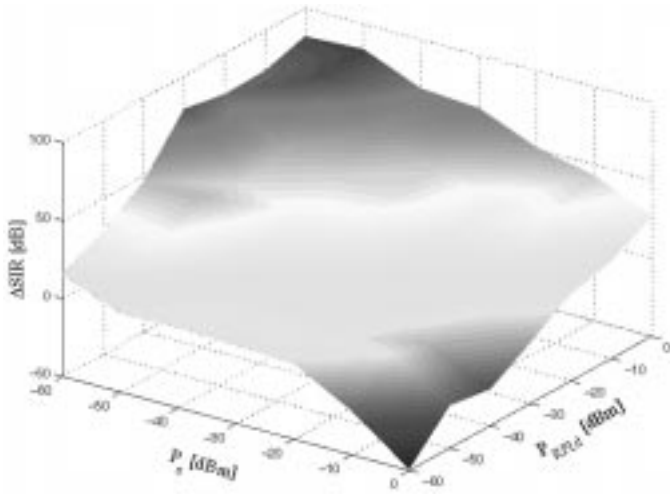


Fig. 7. RFI suppression ΔSIR depending on desired signal's power P_s and DM RFI-ingress power $P_{RFI,d}$ achieved after 10 iterations ($P_{n,c} = -70$ dBm, $P_{n,d} = -70$ dBm, $a_{c2d, dB} = 30$ dB, single-tone interferer).

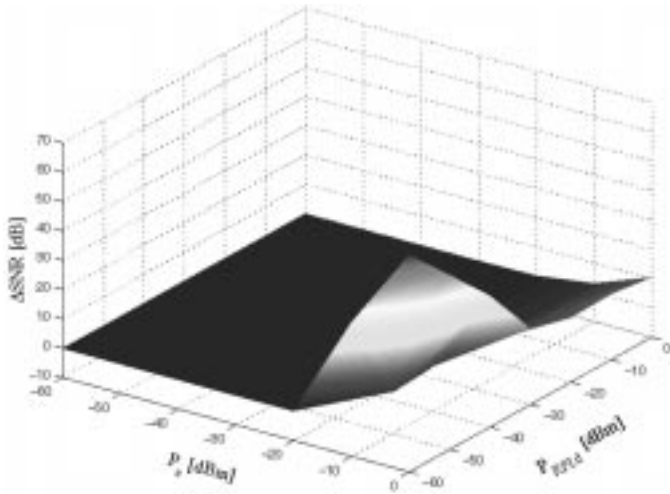


Fig. 8. SNR loss ΔSNR depending on desired signal's power P_s and DM RFI-ingress power $P_{RFI,d}$ achieved after 10 iterations ($P_{n,c} = -70$ dBm, $P_{n,d} = -70$ dBm, $a_{c2d, dB} = 30$ dB, single-tone interferer).

of interest is covered by the worse case of a flat PSD with that maximum value.

B. Results and Discussion

The system-level simulation results presented in this section aim at characterization of the canceller's behavior and performance limits under various operating conditions. The analog part is assumed to be ideal and floating point precision is assumed for the digital algorithm.

1) *Influence of Desired Signal:* Figs. 7 and 8 show the RFI suppression ΔSIR and the SNR loss ΔSNR , respectively, that the canceller achieves after 10 iterations. With rising $P_{RFI,d}$, the RFI component becomes dominant at both DM and CM input. CM reference and quadrature demodulator outputs $q_1(t)$ and $q_2(t)$ are of higher quality, resulting in a higher suppression of stronger RFI (north corner of Fig. 7). Conversely, the interference suppression decreases for $P_{RFI,d} < P_s$ (south corner of Fig. 7).

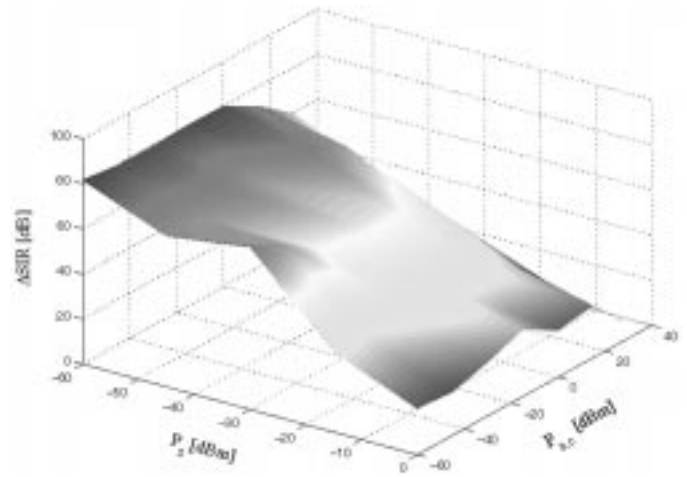


Fig. 9. RFI suppression ΔSIR depending on desired signal's power P_s and broadband CM-noise power $P_{n,c}$ achieved after 10 iterations ($P_{RFI,d} = 0$ dBm, $P_{n,d} = -70$ dBm, $a_{c2d, dB} = 30$ dB, single-tone interferer).

As long as the canceller is able to track the disturber, the weighting coefficients attenuate the CM input signal by a_{c2d} in steady state. The signal component $h_{d2c}(t) \star s(t)$ at the CM input will, thus, appear at the canceller output with a power approximately $2a_{c2d}$ lower than the DM desired signal power P_s . This leakage effect is responsible for the degradation of high SNR in case of strong RFI and strong DM signal (east corner of Fig. 8). For $P_{RFI,d} < P_s$ the canceller loses track of the disturber and may even, depending on the DM to CM coupling function, cancel the DM signal itself (south corner of Figs. 7 and 8). Concerning the balance of the line these results represent the worst case, since maximum coupling ($a_{c2d, dB} = 30$ dB) is assumed. In practice, the canceller would be turned off in this situation.

Summarizing, leakage of the desired signal can be a problem in case both interference and DM signal are strong, the SNR is very high and the DM to CM coupling is strong. Furthermore, the canceller should be inactive in case no or weak RFI (compared with the desired signal's power) is present, which, e.g., can be achieved by thresholding the sampled CM signal power $p(nT)$.

2) *Influence of Broadband CM Noise:* Noise at the CM input has two effects. First, the quality of the RFI reference is degraded, which may reduce the achieved RFI suppression. Second, the noise present at the CM leaks to the canceller output, which may increase the SNR loss. As shown in Fig. 9, the RFI suppression remains sufficient in the target operating area (cf. Fig. 6) as long as the RFI component is dominant at the CM input (west corner of Fig. 9). When the CM noise power is in the same order as the CM RFI power, the suppression decays drastically (north corner of Fig. 9).

Noise at the common mode input can be divided into two components: the part $v_c^{(c)}(t) + h_{d2c}(t) \star v_d^{(c)}(t)$, which is correlated with the DM noise, and the uncorrelated part $v_c^{(u)}(t)$. The SNR loss due to leakage of CM noise that is uncorrelated with the DM signal is clear, as shown in Fig. 10. Correlated CM noise has the potential of cancelling its corresponding DM part in case the coupling is flat and the effective coefficient values, i.e., the coefficients together with an attenuator at the CM input, have

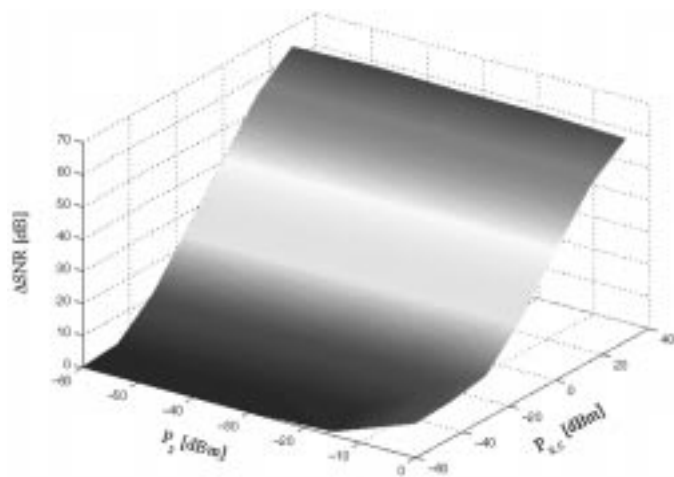


Fig. 10. SNR loss ΔSNR depending on desired signal's power P_s and broadband CM-noise power $P_{n,c}$ achieved after 10 iterations ($P_{RFI,d} = 0$ dBm, $P_{n,d} = -70$ dBm, $a_{c2d,dB} = 30$ dB, single-tone interferer).

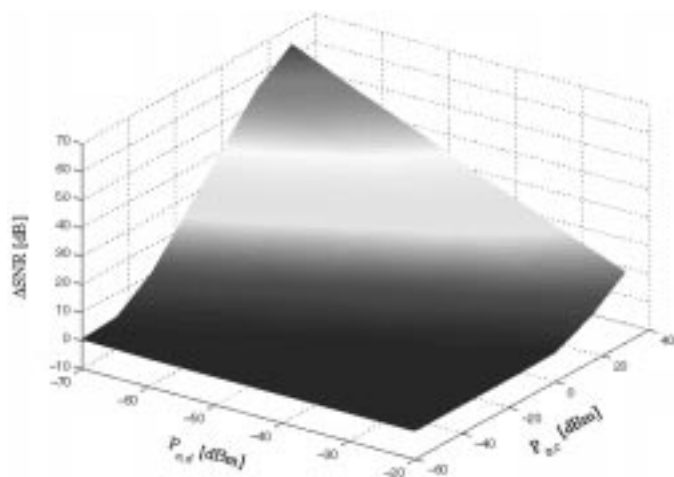


Fig. 11. SNR loss ΔSNR depending on DM-noise power $P_{n,d}$ and broadband CM-noise power $P_{n,c}$ achieved after 10 iterations ($P_{RFI,d} = 0$ dBm, $P_s = -20$ dBm, $a_{c2d,dB} = 30$ dB, single-tone interferer).

converged to $w_1 \approx 1/a_{c2d}$, $w_2 \approx 0$. The output of the PLL is blocked while the CM noise is scaled and subtracted from the DM signal. This scenario, however, is based on the coincidence of several operating conditions that are nontypical in practice. Note that the SNR loss does not depend on P_s except in case of desired signal leakage (south corner of Fig. 10). Fig. 11 shows the influence of DM and CM noise on SNR loss in a typical operating scenario, i.e., $P_{RFI,d} > P_s$. The higher the SNR, the lower is the CM noise power that can be tolerated.

To summarize, noise at the CM input has the potential of severely degrading the SNR at the canceller output, especially for low DM noise power. This is often the case if the SNR is high. If strong, broadband CM noise would be common, the canceller may be designed for specified HAM bands. The CM noise can then be reduced substantially by bandpass filtering.

3) *Influence of RFI Bandwidth:* The behavior of the canceller in case the RFI disturber has (considerable) bandwidth depends strongly on the DM to CM coupling and the 90° -phase splitter. An RFI disturber with small bandwidth, for example if

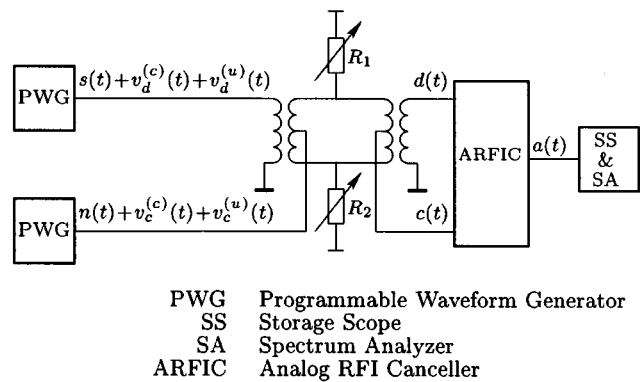


Fig. 12. Block diagram of measurement setup.

the amplitude of the carrier is modulated by speech, is essentially a tone whose amplitude and phase vary slowly compared with its period. The narrowband RFI case is the most common, and what we address in this paper. In case of a broadband disturber, a Hilbert transformer is necessary to generate the two orthogonal signals $u_1(t)$ and $u_2(t)$ instead of the 90° -phase splitter used for tones. In addition, the canceller uses only two coefficients. Thus, it can only realize flat coupling of the CM reference signal, which is sufficient for tones. However, in general the coupling varies over frequency, although often very little. Nonetheless, the canceller's performance degrades with increasing bandwidth in case of nonflat coupling, even with a perfect Hilbert transformer.

V. EXPERIMENTS

A. Controlled Measurements

1) *Setup:* In order to verify the principle, a demonstrator of the canceller has been built according to Fig. 4. A PC equipped with an AD-/DA card with 16 bit resolution has been used to realize the digital part of the canceller. The digital part of the algorithm is implemented in C and a real-time Linux operating kernel assures that the ADCs and DACs are running at a constant frequency of 20 kHz.

Fig. 12 shows a block diagram of the measurement setup. Two transformers are used for combining and separating DM and CM signals, respectively. The unbalance of the line is emulated by the resistors R_1 and R_2 . In our setup, the signal occupies the band from 5.2 to 8.5 MHz, i.e., the second downstream band according to band allocations standardized by ANSI [20] and ETSI [22]. This band overlaps with the 40 m HAM-band (7 MHz to 7.3 MHz). We chose an RFI disturber frequency of 7 MHz. The allocation of signal and disturber is depicted in Fig. 13. Table II summarizes the parameters of the test setup.

2) *Measurement Procedure:* RFI suppression ΔSIR and SNR loss ΔSNR are measured as follows. All signal and noise components, including the RFI disturber, are applied. The canceller is turned on and performs a fixed number of 20 iterations before the coefficients are frozen, which corresponds to the steady state. The canceller's output PSD before and after cancellation yields the achieved RFI suppression ΔSIR as depicted in Fig. 13. Fig. 14 shows the internal canceller signals. For time $t < 0$ the canceller is idle. The weights w_1 and w_2

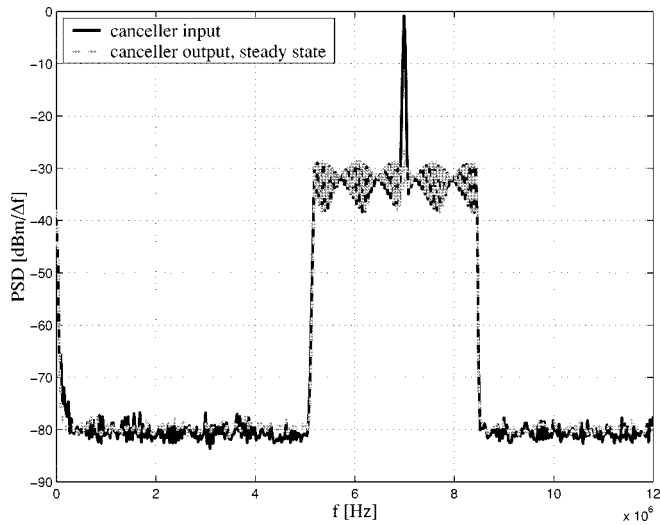


Fig. 13. PSD measured at canceller input and canceller output in steady state, $P_s = -10$ dBm, $P_{\text{RFI},d} = 0$ dBm, $P_{\text{RFI},c} = 30$ dBm, $P_{n,d} = P_{n,c} = -54$ dBm (corresponding PSD: -125 dBm/Hz = -80 dBm/Δf, constant between 0 and 12 MHz), $a_{c2d,dB} = 30$ dB, frequency spacing $\Delta f = 30$ kHz, number of points = 401.

TABLE II
PARAMETERS OF THE MEASUREMENT SETUP

parameter	range	unit
DM signal power P_s	$-\infty \dots 0$	dBm
DM noise PSD $P_{n,d}$	$-125 \dots -63$	dBm/Hz
CM noise PSD $P_{n,c}$	$-125 \dots -65$	dBm/Hz
CM RFI power $P_{\text{RFI},c}$	$-\infty \dots 30$	dBm
DM RFI power $P_{\text{RFI},d}$	$-\infty \dots 0$	dBm
CM to DM coupling $a_{c2d,dB}$	30	dB
RFI disturber's frequency	7	MHz
RFI disturber's bandwidth	$0 \dots 10$	kHz
SNR test-tone's frequency	6	MHz

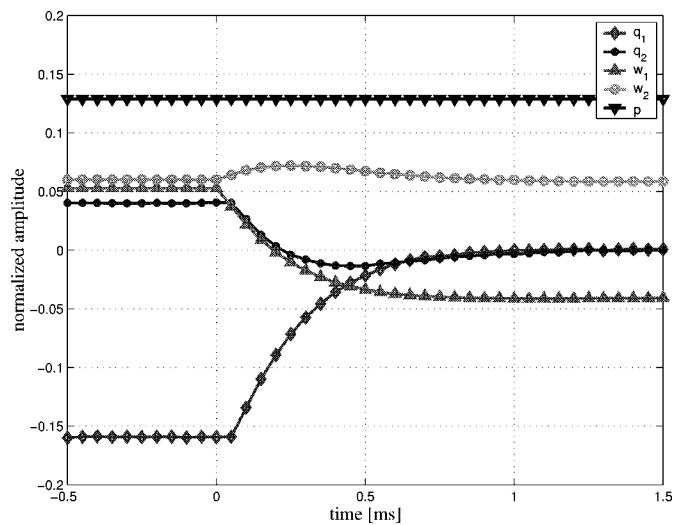


Fig. 14. Canceller signals during adaptation, update frequency $F_S = 20$ kHz, adaptation starts at time = 0 ms.

are set to the levels attained during the offset compensation procedure, as described in Section III-C1. The RFI disturber causes the baseband error-signals q_1 and q_2 to be different from zero. At time instant 0 ms the canceller starts to adapt the weights, which essentially converge after about 20 iterations,

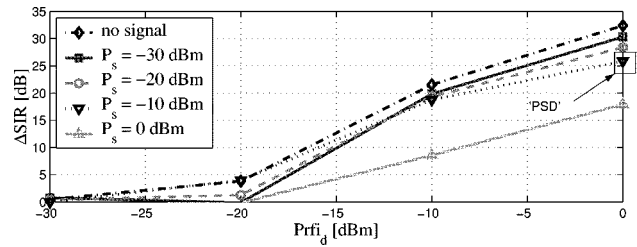


Fig. 15. Measured RFI suppression $\Delta SIR(P_{\text{RFI},d}, P_s)$ versus the power of the RFI disturbance, $P_{n,d} = P_{n,c} = -54$ dBm (corresponding PSD: -125 dBm/Hz, constant between 0 and 12 MHz), $a_{c2d,dB} = 30$ dB, canceller input and output PSD of the operating point labeled "PSD" is shown in Fig. 13.

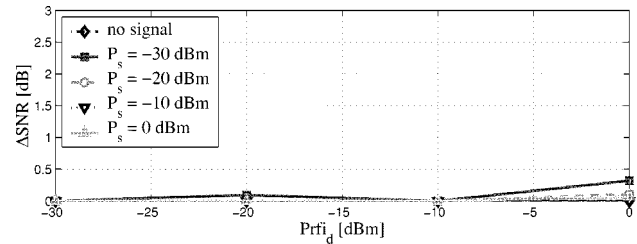


Fig. 16. Measured SNR loss $\Delta SNR(P_{\text{RFI},d}, P_s)$, $P_{n,d} = P_{n,c} = -54$ dBm (corresponding PSD: -125 dBm/Hz, constant between 0 and 12 MHz), $a_{c2d,dB} = 30$ dB.

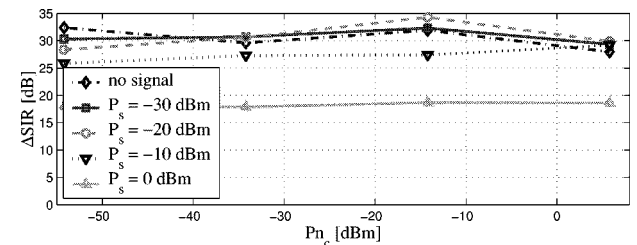


Fig. 17. Influence of CM noise on RFI suppression $\Delta SIR(P_{n,c}, P_s)$, $P_{n,d} = -54$ dBm (corresponding PSD: -125 dBm/Hz, constant between 0 and 12 MHz), $P_{\text{RFI},c} = 30$ dBm, $a_{c2d,dB} = 30$ dB.

which corresponds to 1 ms. The baseband error levels q_1 and q_2 tend toward zero.

In order to measure the SNR loss, the broadband signal is replaced by a test-tone whose frequency lies within the signal band and does not coincide with the RFI disturber. Comparing the strength of that tone with the noise level, and assuming that this relation is the same over the transmit signal band, gives a measure of the SNR loss. This type of measurement is reasonable since the coupling from CM to DM and vice-versa is virtually constant over the frequency band.

a) *Influence of Desired Signal:* Fig. 15 shows the measured RFI suppression ΔSIR for different signal and RFI disturber levels. The RFI suppression rises with increasing RFI power and decreasing signal power. The corresponding SNR loss ΔSNR depicted in Fig. 16 rises with RFI power, which is due to the noise generated by the canceller's multipliers. Quantitatively, the SNR degradation has to be seen in context of the absolute SNR, i.e., we lose 1.5 dB of the total 47 dB. Fig. 13 shows the PSD of the canceller input and output signals in steady state.

b) *Influence of Broadband CM Noise:* Figs. 17 and 18 show the influence of broadband CM noise on ΔSIR

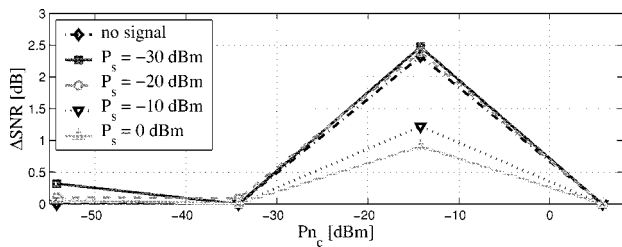


Fig. 18. Influence of CM noise on SNR loss $\Delta SNR(P_{n,c}, P_s)$, $P_{n,d} = -54$ dBm (corresponding PSD: -125 dBm/Hz, constant between 0 and 12 MHz), $P_{RFI,c} = 30$ dBm, $a_{c2d,dB} = 30$ dB.

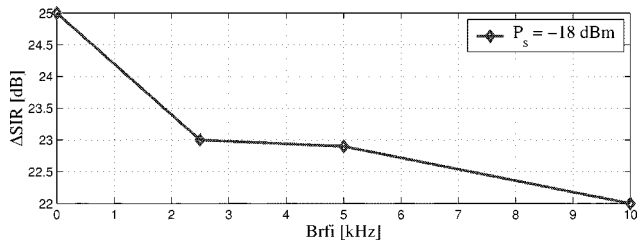


Fig. 19. Influence of RFI disturber's bandwidth on RFI suppression. Please note the scale on the y axis. $P_{n,d} = -125$ dBm/Hz, $P_{n,c} = -125$ dBm/Hz, $P_{RFI,c} = 30$ dBm, $a_{c2d,dB} = 30$ dB.

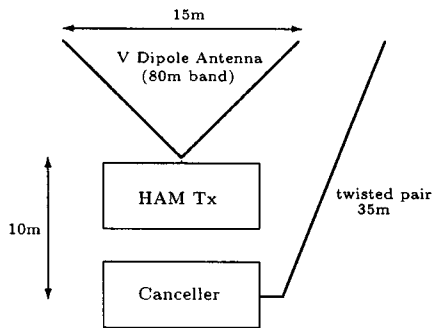


Fig. 20. Experimental setup.

and ΔSNR , respectively. The RFI suppression decreases slightly with rising CM noise. The SNR loss increases up to a CM noise power of -15 dBm because CM noise leaks to the canceller output. Note that the SNR loss decreases for stronger CM noise levels, since the DM noise component that is coupled in from the CM due to the line unbalance is reduced by canceller. This effect occurs because of the flat coupling between CM and DM and the special values of the coefficients ($w_1 \approx 1/a_{c2d}$, $w_2 \approx 0$), and has, as already discussed in Section IV-B2, only limited practical relevance.

c) *Influence of RFI Bandwidth:* The SNR suppression decays moderately with increasing RFI disturber bandwidth as shown in Fig. 19. Since the coupling is flat in this frequency band, Fig. 19 essentially shows the performance of the 90° -phase splitter.

B. HAM-Ingress Experiments

A second series of experiments examines the canceller's performance in case of real HAM ingress. The experimental setup, shown in Fig. 20, has been chosen to resemble a real scenario as closely as possible, given the constraints at the measurement

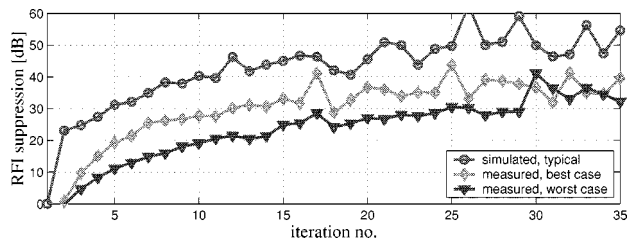


Fig. 21. Measured canceller performance compared with simulation: evolution of RFI suppression—best case and worst case of the measurement series and typical simulation result.

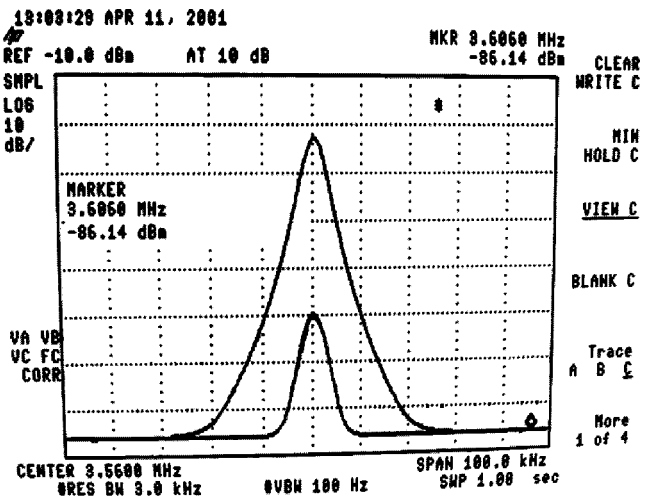


Fig. 22. Real HAM ingress: screen shot showing the steady state suppression.

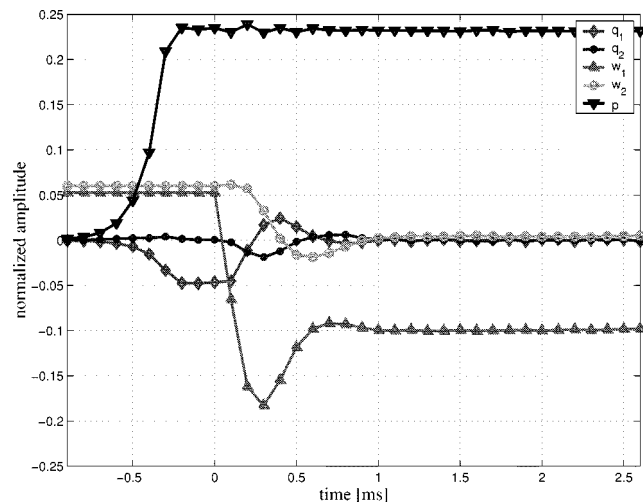


Fig. 23. Canceller signals during adaptation to real HAM ingress (1 ms ramp-up time), adaptation starts at time = 0 ms, the sampling frequency F_s is 10 kHz.

site. The field measurements were done with a sampling frequency F_s of 10 kHz. The HAM-signal was in the 3.5–3.7 MHz HAM-band. The measured RFI disturbance suppression during convergence is compared with simulations in Fig. 21. Fig. 22 shows a screen shot of the steady-state suppression of 35 dB. The canceller signals, depicted in Fig. 23, show essentially the same behavior as in the laboratory measurements. Note that we started the canceller manually (at time = 0 ms) as opposed to activating it when the RFI power exceeds a certain threshold.

VI. CONCLUSION

RFI cancellation before the receiver's ADC, i.e., in the analog domain, is both necessary and difficult for broadband wireline transmission systems. The HAM disturbance is bursty and exhibits high power levels. The main goal of the analog interference canceller is to prevent the ADC from overloading.

An adaptive mixed-signal cancellation scheme, and an example implementation, is proposed and detailed. It generates an interference-cancelling signal of several MHz, while the adaptive algorithm operates at a rate of some kilohertz. This is essentially achieved by splitting the RLS algorithm into an analog and a digital part, where the high-frequency signal processing is analog. Simulation results, confirmed by demonstrator measurements, are presented. The canceller needs to be, and is, fast enough to protect data transmission over copper twisted pairs from HAM radio interference. Once adjusted, the canceller achieves a narrowband interference suppression of about 35 dB. However, we do not propose to aim at an exceptionally high suppression in the analog domain. The goal is to protect the receiver's ADC with reasonable implementation effort. Further suppression can be done more efficiently in digital domain.

APPENDIX

TWO-COEFFICIENT MIXED-SIGNAL RLS ALGORITHM

We base our analysis on the following model of the DM signal:

$$d(t) = \mathbf{w}_o^T(t)\mathbf{u}(t) + s(t) + v_d(t). \quad (16)$$

Since the expectation of the unobservable desired signal $s(t)$ and the uncorrelated noise component $v_d(t)$ is zero, i.e., $E\{s(t) + v_d(t)\} = 0$, we postulate

$$r(t) = \mathbf{w}^T(t)\mathbf{u}(t) \quad (17)$$

as the model of interest. The estimation error or residual error $e(t)$ is given by

$$e(t) = d(t) - r(t) = d(t) - \mathbf{w}^T(t)\mathbf{u}(t). \quad (18)$$

We define the cost function

$$\mathcal{E}[n] = \frac{1}{T} \int_{t=0}^{nT} \lambda^{(nT-t)/T} e^2(t) dt \quad (19)$$

where λ is a forgetting factor weighting recent data higher than older data. Note that the coefficients $w_1(t)$ and $w_2(t)$ remain fixed during the entire observation interval $0 \leq t < nT$ i.e., $\mathbf{w}(t) = \mathbf{w}[n]$ for $0 \leq t < nT$. In order to minimize the cost function, we define the k th component of the gradient vector $\nabla_k \mathcal{E}[n]$ as the derivative of the cost function with respect to the k th coefficient $w_k(t)$, i.e.,

$$\nabla_k \mathcal{E}[n] = \frac{\partial \mathcal{E}[n]}{\partial w_k(t)}, \quad k = 1, 2. \quad (20)$$

Substituting (18) and (19) in (20) and differentiating $e(t)$ with respect to $w_k(t)$ yields

$$\nabla_k \mathcal{E}[n] = -\frac{2}{T} \int_{t=0}^{nT} \lambda^{(nT-t)/T} e(t) u_k(t) dt, \quad k = 1, 2. \quad (21)$$

Let $e_{\min}(t)$ denote the special estimation error function minimizing (19) by choosing the optimum coefficients $\hat{w}_k(t) = \hat{w}_k[n]$ for $0 \leq t < nT$, i.e.,

$$\begin{aligned} e_{\min}(t) &= d(t) - \hat{\mathbf{w}}^T[n]\mathbf{u}(t) \\ &= d(t) - \sum_{k=1}^2 \hat{w}_k[n] u_k(t). \end{aligned} \quad (22)$$

Since the estimation error function $e_{\min}(t)$ minimizes (19), the corresponding derivatives $\nabla_k \mathcal{E}[n]$, $k = 1, 2$ are zero. Thus changing the index k to l in (22) and substituting into (21) yields

$$\begin{aligned} \frac{1}{T} \int_{t=0}^{nT} \lambda^{(nT-t)/T} d(t) u_k(t) dt \\ = \sum_{l=1}^2 \hat{w}_l[n] \frac{1}{T} \int_{t=0}^{nT} \lambda^{(nT-t)/T} u_k(t) u_l(t) dt \end{aligned} \quad (23)$$

which can be written more compactly as

$$\underbrace{\begin{bmatrix} z_1[n] \\ z_2[n] \end{bmatrix}}_{\mathbf{z}[n]} = \underbrace{\begin{bmatrix} \Phi_{1,1}[n] & \Phi_{1,2}[n] \\ \Phi_{2,1}[n] & \Phi_{2,2}[n] \end{bmatrix}}_{\mathbf{\Phi}[n]} \underbrace{\begin{bmatrix} \hat{w}_1[n] \\ \hat{w}_2[n] \end{bmatrix}}_{\hat{\mathbf{w}}[n]} \quad (24)$$

where

$$z_k[n] = \frac{1}{T} \int_{t=0}^{nT} \lambda^{(nT-t)/T} d(t) u_k(t) dt \quad (25)$$

and

$$\Phi_{k,l}[n] = \frac{1}{T} \int_{t=0}^{nT} \lambda^{(nT-t)/T} u_k(t) u_l(t) dt. \quad (26)$$

Now we want to find a recursive expression for $\mathbf{z}[n]$ which can be done easily by splitting the integral in (25), i.e.,

$$\begin{aligned} z[n] &= \lambda \frac{1}{T} \int_{t=0}^{(n-1)T} \lambda^{(nT-t-T)/T} d(t) \mathbf{u}(t) dt \\ &\quad + \frac{1}{T} \int_{t=(n-1)T}^{nT} \lambda^{(nT-t)/T} d(t) \mathbf{u}(t) dt \\ &= \lambda z[n-1] + \frac{1}{T} \int_{t=(n-1)T}^{nT} \lambda^{(nT-t)/T} d(t) \mathbf{u}(t) dt. \end{aligned} \quad (27)$$

Accordingly, we may express the entire correlation matrix recursively

$$\mathbf{\Phi}[n] = \lambda \mathbf{\Phi}[n-1] + \frac{1}{T} \int_{t=(n-1)T}^{nT} \lambda^{(nT-t)/T} \mathbf{u}(t) \mathbf{u}^T(t) dt. \quad (28)$$

From (24), the coefficient vector can be written as

$$\hat{\mathbf{w}}[n] = \mathbf{\Phi}^{-1}[n] \mathbf{z}[n]. \quad (29)$$

Substituting (27) and (28) in (29) yields

$$\begin{aligned} \hat{\mathbf{w}}[n] &= \left(\lambda \mathbf{\Phi}[n-1] + \frac{1}{T} \int_{t=(n-1)T}^{nT} \lambda^{(nT-t)/T} \mathbf{u}(t) \mathbf{u}^T(t) dt \right)^{-1} \\ &\quad \cdot \left(\lambda z[n-1] + \frac{1}{T} \int_{t=(n-1)T}^{nT} \lambda^{(nT-t)/T} d(t) \mathbf{u}(t) dt \right). \end{aligned} \quad (30)$$

After a few basic manipulations we arrive at

$$\begin{aligned} \hat{\mathbf{w}}[n] &= \hat{\mathbf{w}}[n-1] \\ &+ \left(\lambda \Phi[n-1] + \frac{1}{T} \int_{t=(n-1)T}^{nT} \lambda^{(nT-t)/T} \right. \\ &\quad \cdot \mathbf{u}(t) \mathbf{u}^T(t) dt \left. \right)^{-1} \\ &\cdot \left(\frac{1}{T} \int_{t=(n-1)T}^{nT} \lambda^{(nT-t)/T} \mathbf{u}(t) \right. \\ &\quad \cdot (d(t) - \hat{\mathbf{w}}^T[n-1] \mathbf{u}(t)) dt \left. \right). \end{aligned} \quad (31)$$

Since the reference signal components $u_1(t)$ and $u_2(t)$ are orthogonal, two assumptions hold. First, $u_1(t)$ and $u_2(t)$ have the same time-averaged power

$$\begin{aligned} \int_{t=0}^{nT} \lambda^{(nT-t)/T} u_1(t) u_1(t) dt &= \int_{t=0}^{nT} \lambda^{(nT-t)/T} u_2(t) u_2(t) dt \\ &= P[n]. \end{aligned} \quad (32)$$

Second, the time-averaged product of $u_1(t)$ and $u_2(t)$ is zero

$$\int_{t=0}^{nT} \lambda^{(nT-t)/T} u_1(t) u_2(t) dt = 0. \quad (33)$$

Using (32) and (33), we may rewrite (28) as

$$P[n] \mathcal{I} = \left(\lambda P[n-1] + \frac{1}{T} \int_{t=(n-1)T}^{nT} \lambda^{(nT-t)/T} u_k^2(t) dt \right) \mathcal{I} \quad (34)$$

where \mathcal{I} is the identity matrix. Either $u_1(t)$ or $u_2(t)$ can be used inside the integral since they have the same average power according to (32). Rewriting (31) taking into account (34) yields the mixed-signal recursive expression for the weights

$$\hat{\mathbf{w}}[n] = \hat{\mathbf{w}}[n-1] + \frac{1}{P[n]} \frac{1}{T} \int_{t=(n-1)T}^{nT} \lambda^{(nT-t)/T} \mathbf{u}(t) \xi(t) dt \quad (35)$$

where $\xi(t)$ is the *a priori* estimation error

$$\xi(t) = d(t) - \hat{\mathbf{w}}^T[n-1] \mathbf{u}(t), \quad (n-1)T \leq t < nT. \quad (36)$$

The integral in (35) represents the convolution of $(1/T)\lambda^{t/T}$ and $\mathbf{u}(t)\xi(t)$. Thus, we can rewrite (35) as

$$\begin{aligned} \hat{\mathbf{w}}[n] &= \hat{\mathbf{w}}[n-1] + \frac{1}{P[n]} h_{\lambda a}(nT) \star (\mathbf{u}(nT) \xi(nT)) \\ &= \hat{\mathbf{w}}[n-1] + \frac{1}{P[n]} \mathbf{q}(nT) \end{aligned} \quad (37)$$

where $h_{\lambda a}(t)$ is the optimum (in the sense of minimizing $\mathcal{E}[n]$) low-pass filter impulse response

$$h_{\lambda a}(t) = \begin{cases} \frac{1}{T} \lambda^{t/T} & 0 \leq t \leq T \\ 0 & \text{otherwise} \end{cases} \quad (38)$$

and $\mathbf{q}(t)$ is the baseband error signal vector, i.e.,

$$\mathbf{q}(t) = \begin{bmatrix} q_1(t) \\ q_2(t) \end{bmatrix} = \begin{bmatrix} h_{\lambda a}(t) \star (u_1(t) \xi(t)) \\ h_{\lambda a}(t) \star (u_2(t) \xi(t)) \end{bmatrix}. \quad (39)$$

The input signal power measure $P[n]$ can be recursively updated by

$$P[n] = \lambda P[n-1] + \frac{1}{T} \int_{t=(n-1)T}^{nT} \lambda^{(nT-t)/T} u_k^2(t) dt. \quad (40)$$

Again the integral represents the convolution, i.e., we may rewrite (40)

$$\begin{aligned} P[n] &= \lambda P[n-1] + h_{\lambda a}(nT) \star u_k^2(nT) \\ &= \lambda P[n-1] + p(nT) \end{aligned} \quad (41)$$

where $p(t)$ is the CM reference power signal

$$p(t) = h_{\lambda a}(t) \star u_k^2(t) = h_{\lambda a}(t) \star c^2(t). \quad (42)$$

This holds since $u_k(t)$ are just time-shifted versions of the sinusoidal CM input signal $c(t)$. Thus, all three signals have the same average power.

ACKNOWLEDGMENT

The authors would like to thank T. Lundberg (EURAB, Sweden), M. Isaksson (Telia Research AB, Sweden) and A. Scholtz (Vienna University of Technology, Austria) for providing the opportunity to carry out real HAM ingress measurements. They are grateful to M. Lončar and W. Henkel (both FTW, Austria) for their valuable support.

REFERENCES

- [1] L. de Clercq, M. Peeters, S. Schelstraete, and T. Pollet, "Mitigation of radio interference in xDSL transmission," *IEEE Commun. Mag.*, vol. 38, no. 3, pp. 168–173, Mar. 2000.
- [2] K. T. Foster and J. W. Cook, "The Radio Frequency Interference (RFI) environment for very high-rate transmission over metallic access wire-pairs," ANSI Contribution, T1E1.4/95-020, 1995.
- [3] K. T. Foster, "Practical measurements of the levels of induced RFI from amateur radio transmissions on various lengths of three types of drop-wiring commonly found in BTs access network," ANSI Contribution, T1E1.4/95-097, 1995.
- [4] M. Sehlstedt, "RFI cancellation in VDSL," Master thesis, LTU-EX-00 327-SE, Luleå University of Technology, Luleå, Sweden, 2000.
- [5] J. Bingham, J. M. Cioffi, and M. Mallory, "Digital RFI cancellation with SDMT," ANSI Contribution, T1E1.4/96-083, 1996.
- [6] F. Sjöberg, R. Nilsson, N. Grip, P. O. Börjesson, S. K. Wilson, and P. Ödling, "Digital RFI suppression in DMT-based VDSL systems," in *Proc. ICT98*, vol. 2, 1998, pp. 189–193.
- [7] T. Yeap, "A digital common-mode noise canceller for twisted-pair cable," ANSI Contribution, T1E1.4/99-260, 1999.
- [8] R. Nilsson, F. Sjöberg, and J. P. LeBlanc, "A narrow-band interference canceller for OFDM-based systems," in *Proc. EPMCC01*, Session 17.3, Vienna, Austria, Feb. 2001.
- [9] D. Harman, G. H. Im, and J. J. Werner, "Steady-state performance and blind training of a DFE in the presence of RF interference," ANSI Contribution, T1E1.4/97-104, 1997.
- [10] D. I. Pazaitis, J. Maris, S. Vernaide, M. Engels, and I. Bolsens, "Equalization and radio frequency interference cancellation in broadband twisted pair receivers," in *Proc. GLOBECOM98*, vol. 6, 1998, pp. 3503–3508.
- [11] J. M. Cioffi, M. Mallory, and J. Bingham, "Analog RF cancellation with SDMT," ANSI Contribution, T1E1.4/96-084, 1996.
- [12] N. P. Sands, E. Naviaskey, W. Evans, M. Mengele, K. Faison, C. Frost, M. Casas, and M. Williams, "An integrated analog front-end for VDSL," *Dig. Technical Papers ISSCC99*, pp. 246–247, 1999.
- [13] T. Magesacher, P. Ödling, T. Nordström, T. Lundberg, M. Isaksson, and P. O. Börjesson, "An adaptive mixed-signal narrowband interference canceller for wireline transmission systems," in *Proc. IEEE Int. Symp. Circuits and Systems*, vol. IV, Sydney, Australia, May 2001, pp. 450–453.

- [14] B. Widrow, "Adaptive noise cancelling: principles and applications," *Proc. IEEE*, vol. 63, pp. 1692–1716, Dec. 1975.
- [15] S. Haykin, *Adaptive Filter Theory*, 3rd ed. Englewood Cliffs, NJ: Prentice-Hall, 1996.
- [16] F. J. Kub and E. W. Justh, "Analog CMOS implementation of high frequency least-mean square error learning circuit," *IEEE J. Solid-State Circuits*, vol. 30, pp. 1391–1398, Dec. 1995.
- [17] T. Linder, H. Zojer, and B. Seger, "Fully analogue LMS adaptive notch filter in BiCMOS technology," *IEEE J. Solid-State Circuits*, vol. 31, pp. 81–89, Jan. 1996.
- [18] T. Magesacher, S. Haar, R. Zukunft, P. Ödler, T. Nordström, and P. O. Börjesson, "Splitting the recursive least-squares algorithm," in *Proc. 6th Int. Symp. Signal Processing and Its Applications ISSPA2001*, vol. 1, Kuala Lumpur, Malaysia, Aug. 2001, pp. 319–322.
- [19] B. R. Saltzberg, "Comparison of single-carrier and multitone modulation for ADSL applications," *IEEE Commun. Mag.*, vol. 36, pp. 114–121, Nov. 1998.
- [20] ANSI T1e1.4, "Very-High-Bit-Rate Digital Subscriber Line (VDSL) metallic interface Part 1: Functional requirement and common specification," ANSI, T1E1.4/2000-009R3, Feb. 2001.
- [21] ETSI TM6, "Transmission and Multiplexing (TM); Access transmission systems on metallic access cables; Very High Speed Digital Subscriber Line (VDSL); Part 1: Functional requirements," ETSI, TS 101 270-1, Version 1.1.6, Aug. 1999.
- [22] ETSI TM6, "Transmission and Multiplexing (TM); Access transmission systems on metallic access cables; Very High Speed Digital Subscriber Line (VDSL); Part 2: Transceiver specification," ETSI, TS 101 270-2, Version 1.1.5, Dec. 2000.



Per Ödler (S'90–A'95–M'00–SM'01) was born in Örnsköldsvik, Sweden, in November 1966. He received the M.S.E.E. degree, in 1989, a licentiate of engineering, in 1993, and the Ph.D. degree in signal processing, in 1995, all from Luleå University of Technology, Sweden. In 2000, he received the Docent degree from Lund Institute of Technology, Sweden.

He was an Assistant Professor at Luleå University until 1999, when he moved from the arctic north of Luleå to historic Vienna, as Key Researcher at the Telecommunications Research Center Vienna, Austria (ftw). There he spent three years advising graduate students and industry, while researching broadband Internet access and services. He is, since 2001, an Associate Professor at the Department of Electrosience, Lund Institute of Technology, stationed at Ericsson Telecom AB, Stockholm, as a part of a cooperation. Having researched cooperatively with industry over more than ten years, he is developing broadband Internet communication systems over radio and twisted copper pairs, and advising Ph.D. students in these areas. His research interests focus on signal processing and statistical communications, but range to the convergence of data- and telecommunications and technical regulatory issues.



Per Ola Börjesson (S'70–M'80–SM'01) was born in Karlshamn, Sweden, in 1945. He received the M.Sc. degree in electrical engineering, in 1970, and the Ph.D. degree in telecommunication theory, in 1980, both from Lund Institute of Technology (LTH), Lund, Sweden. In 1983, he received the degree of Docent in Telecommunication Theory.

Since 1998, he has been a Professor of Signal Processing at Lund University, and between 1988 and 1998, he was Professor of Signal Processing at Luleå University of Technology, Sweden. His primary research interest is in high performance communication systems, in particular, high data rate wireless and twisted pair systems. He is presently researching signal processing techniques in communication systems that use orthogonal frequency division multiplexing (OFDM) or discrete multitone (DMT) modulation. He emphasizes the interaction between models and real systems, from the creation of application-oriented models based on system knowledge to the implementation and evaluation of algorithms.



Thomas Magesacher (S'01) was born in Friesach, Austria, in 1974. He received the Dipl.-Ing. degree, in 1998 from Graz Technical University, Austria. He is a Ph.D. student of BridgeLab, Institute for Integrated Circuits of Munich University of Technology, Germany.

Since 1998, he has been with Infineon Technologies, stationed in Austria, Germany, and Israel, focusing on high speed data transmission systems over copper twisted pairs (xDSL) in Austria, Germany, and Israel. Currently, he is at the Telecommunications Research Center Vienna (ftw), Austria, working in the field of digital signal processing for wireline communications. His research interests are digital modulation techniques, adaptive and mixed-signal processing.



Tomas Nordström (S'88–A'95–M'00–SM'01) was born in Härnösand, Sweden, in 1963. He received the M.S.E.E. degree, in 1988, the licentiate degree, in 1991, and the Ph.D. degree, in 1995, all from Luleå University of Technology, Sweden.

Currently, he is a Key Researcher and Project Manager at the Telecommunications Research Center Vienna (ftw), Austria. During 1995 and 1996, he was an Assistant Professor at Luleå University of Technology researching computer architectures, neural networks, and signal processing. Between 1996 and 1999, he was with Telia Research (the research branch of the Swedish incumbent telephone operator) where he developed broadband Internet communication over twisted copper pairs. He was instrumental in the development of the Zipper-VDSL concept (contributed to the standardization of VDSL in ETSI, ANSI, and ITU) and in the design of the Zipper-VDSL prototype modems. In addition, he was Telia's national expert on speaker verification. In December 1999, he joined the Telecommunications Research Center Vienna (FTW), where he is the project manager of the "Broadband access over wire" group. He is also a consultant covering design, development, and deployment of DSL modems.